

Synchronization of nanowire-based spin Hall nano-oscillators

Biao Jiang(姜彪)1, Wen-Jun Zhang(张文君)2, Mehran Khan Alam1, Shu-Yun Yu(于淑云)1, Guang-Bing Han(韩广兵)1, Guo-Lei Liu(刘国磊)1, Shi-Shen Yan(颜世申)1, and Shi-Shou Kang(康仕寿)1,†

Citation: Chin. Phys. B, 2022, 31 (7): 077503 DOI: 10.1088/1674-1056/ /ac560a
Journal homepage: http://cpb.iphy.ac.cn; http://iopscience.iop.org/cpb

What follows is a list of articles you may be interested in

Interaction region of magnon-mediated spin torques and novel magnetic states

Zai-Dong Li(李再东), Qi-Qi Guo(郭奇奇), Yong Guo(郭永), Peng-Bin He(贺鹏斌), and Wu-Ming Liu(刘伍明)
Chin. Phys. B, 2021, 30 (**10**): 107506. DOI: 10.1088/1674-1056/ac04a8

Magnetic excitations of diagonally coupled checkerboards

Tingting Yan(颜婷婷), Shangjian Jin(金尚健), Zijian Xiong(熊梓健), Jun Li(李军), and Dao-Xin Yao(姚道新)
Chin. Phys. B, 2021, 30 (**10**): 107505. DOI: 10.1088/1674-1056/ac1b94

Magnon bands in twisted bilayer honeycomb quantum magnets

Xingchuan Zhu(朱兴川), Huaiming Guo(郭怀明), and Shiping Feng(冯世平)
Chin. Phys. B, 2021, 30 (**7**): 077505. DOI: 10.1088/1674-1056/abeee5

Origin of itinerant ferromagnetism in two-dimensional Fe_3GeTe_2

Xi Chen(陈熙), Zheng-Zhe Lin(林正喆), and Li-Rong Cheng(程丽蓉)
Chin. Phys. B, 2021, 30 (**4**): 047502. DOI: 10.1088/1674-1056/abd164

Spin waves and transverse domain walls driven by spin waves: Role of damping

Zi-Xiang Zhao(赵梓翔), Peng-Bin He(贺鹏斌), Meng-Qiu Cai(蔡孟秋), Zai-Dong Li(李再东)
Chin. Phys. B, 2020, 29 (**7**): 077502. DOI: 10.1088/1674-1056/ab90e5

Synchronization of nanowire-based spin Hall nano-oscillators

Biao Jiang(姜彪)[1], Wen-Jun Zhang(张文君)[2], Mehran Khan Alam[1], Shu-Yun Yu(于淑云)[1], Guang-Bing Han(韩广兵)[1], Guo-Lei Liu(刘国磊)[1], Shi-Shen Yan(颜世申)[1], and Shi-Shou Kang(康仕寿)[1,†]

[1] *School of Physics, State Key Laboratory of Crystal Materials, Shandong University, Jinan* 250100, *China*
[2] *Department of Physics and Electronic Science, Weifang University, Weifang* 261061, *China*

(Received 21 December 2021; revised manuscript received 11 February 2022; accepted manuscript online 17 February 2022)

The synchronization of the spin Hall nano-oscillator (SHNO) device driven by the pure spin current has been investigated with micromagnetic simulations. It was found that the power spectra of nanowire-based SHNO devices can be synchronized by varying the current flowing in the heavy metal (HM) layer. The synchronized signals have relatively high power and narrow linewidth, favoring the potential applications. We also found that the synchronized spectra are strongly dependent on both the number and length of nanowires. Moreover, a periodic modulation of power spectra can be obtained by introducing interfacial Dzyaloshinskii–Moriya interaction (iDMI). Our findings could enrich the current understanding of spin dynamics driven by the pure spin current. Further, it could help to design novel spintronic devices.

Keywords: spin Hall nano-oscillators, synchronization, Dzyaloshinskii–Moriya interaction, spin wave

PACS: 75.75.–c, 75.30.Ds, 07.55.–w **DOI:** 10.1088/1674-1056/ac560a

1. Introduction

Spin current or spin-polarized current[1–3] can drive the magnetization dynamics by transferring of spin angular momentum, resulting in transfer torque, magnetic random-access memory (MRAM), and spin nano-oscillator,[4–16] which can be widely used in future information storage, computing, and reading areas. Generally, the spin nano-oscillators can be divided into spin-torque nano-oscillator (STNO) and spin Hall nano-oscillator (SHNO). The former is the polarization current that directly flows into the magnetic layer and generates microwave through giant magnetoresistance (GMR) effect and tunneling magnetoresistance (TMR).[7,8] And the latter is due to the pure spin current generated by the spin Hall effect (SHE) in the heavy metal (NM) layer, which brings negative damping to the adjacent magnetic layer and realizes the stable magnetization oscillation. Finally, the microwave emission is generated through the magnetic layer's anisotropic magnetoresistance (AMR) effect.[9–11] Compared to STNO, SHNO has no additional effects such as Joule heat caused by the direct charge flow and potential damage to the device. Meanwhile, SHNO has a narrower linewidth,[7–9,12–14] making it more suitable for applications. Moreover, SHNO is relatively easier to be nano fabricated and optically detected.[9,12,13] However, because the AMR effect of SHNO is generally small, its output power is relatively low, usually in the order of pW.[17–19] Since the high-quality signal is desired in future applications, further enhancing the power and reducing the linewidth of the signal is necessary. Many progress has been achieved, including using external devices, such as adding magnetic tunnel junctions (MTJs) structure on the SHNO structure,[20,21] synchronization of multiple devices,[17,22–28] *etc*. In principle, the synchronized power will be remarkably increased by nearly N^2 times for the multiple devices with the number of N. Meanwhile, the white noise and linewidth will decrease significantly with N.[1,22] Since a few works have been devoted to one-dimensional nanowire-based SHNO, it is interesting to investigate further its synchronization behavior for future applications with high output signals. Furthermore, the geometric constraints of one-dimensional nanowires can effectively suppress the nonlinear magnon scattering, which significantly expands the active region of SHNO for stable magnetization oscillation.[1,29] Moreover, as a one-dimensional structure, nanowire-based SHNO has the potential for optimization and space-saving.[29–34] For example, the parallel edge of nanowires can be changed to inclined edge to reduce the phase noise of signal.[33] In this work, we focus on the dynamical behavior of a one-dimensional nanowire oscillator using micromagnetic simulations. We identify that the synchronization is realized by tuning the frequencies and phases of both bulk and edge modes. We further demonstrated that the output power of the synchronized SHNO significantly increases with the number of devices. Moreover, the influence of interfacial Dzyaloshinskii–Moriya interaction (iDMI) on synchronization has been investigated and discussed. It will be of great significance for the developing nano logic devices and neuromorphic computing in the future.[32–34]

2. Results and discussion

First, we have designed a series of nanowire-based SHNO consisting of Pt (6 nm)/permalloy (Py) (2 nm) with different geometries. As shown in Fig. 1(a), the distance between adja-

†Corresponding author. E-mail: skang@sdu.edu.cn

© 2022 Chinese Physical Society and IOP Publishing Ltd

cent nanowires is 260 nm, and the nanowire width is 60 nm. The size of the whole structure in the x–y plane is 3000 nm ×3000 nm. The in-plane field angle was fixed at $\theta = 26°$ to ensure sufficient electrical sensitivity to the auto-oscillation signal. In contrast, the out-of-plane field angle $\varphi = 292°$ was chosen in a way to achieve large positive nonlinearity in the active nanowire region.[35–37] The spin current generated in the Pt layer flows vertically to the Py layer, subsequently, driving the stable oscillation in the upper ferromagnetic layer.

The micromagnetic calculations are carried out using the mumax3 solver[38] with the current density and Oersted field obtained from the COMSOL simulations. In general, the magnetization dynamics is described by the LLG equation by taking SHE into account[13]

$$\frac{\mathrm{d}\boldsymbol{M}}{\mathrm{d}t} = -\gamma_0 \boldsymbol{M} \times \boldsymbol{H}_{\mathrm{eff}} + \frac{\alpha}{M_{\mathrm{s}}} \boldsymbol{M} \times \frac{\mathrm{d}\boldsymbol{M}}{\mathrm{d}t} + \tau_{\mathrm{SHE}},$$

where $\boldsymbol{M}$ and $\boldsymbol{H}_{\mathrm{eff}}$ are the magnetization and the effective field vectors of the ferromagnet, respectively. α, M_{S}, and γ_0 are the Gilbert damping, the saturation magnetization, and the gyromagnetic ratio, respectively. $\boldsymbol{H}_{\mathrm{eff}}$ represents the magnetocrystalline anisotropy, the Oersted field, and the random thermal field. τ_{SHE} is the SHE item and proportional to

$$\frac{\Theta_{\mathrm{SH}} J(x,y)}{eM_{\mathrm{s}}} \boldsymbol{M} \times \boldsymbol{M} \times \sigma.$$

Here, $\Theta_{\mathrm{SH}} = 0.08$ is the spin Hall angle of Pt, and $J(x,y)$ is the current density in Pt. The parameters for our permalloy are: exchange constant 1.3×10^{11} J/m, Gilbert damping 0.02, and saturation magnetization 650×10^3 A/m, respectively.[13] The simulated cell size $\Delta x \Delta y \Delta z$ is 2.5 nm×2.5 nm×2 nm. Since the current was dominant in the heavy metal layer, the contribution of the current in the magnetic layer can be nearly neglected. All simulations were carried out at room temperature. Magnetic coupling was built into our simulations.

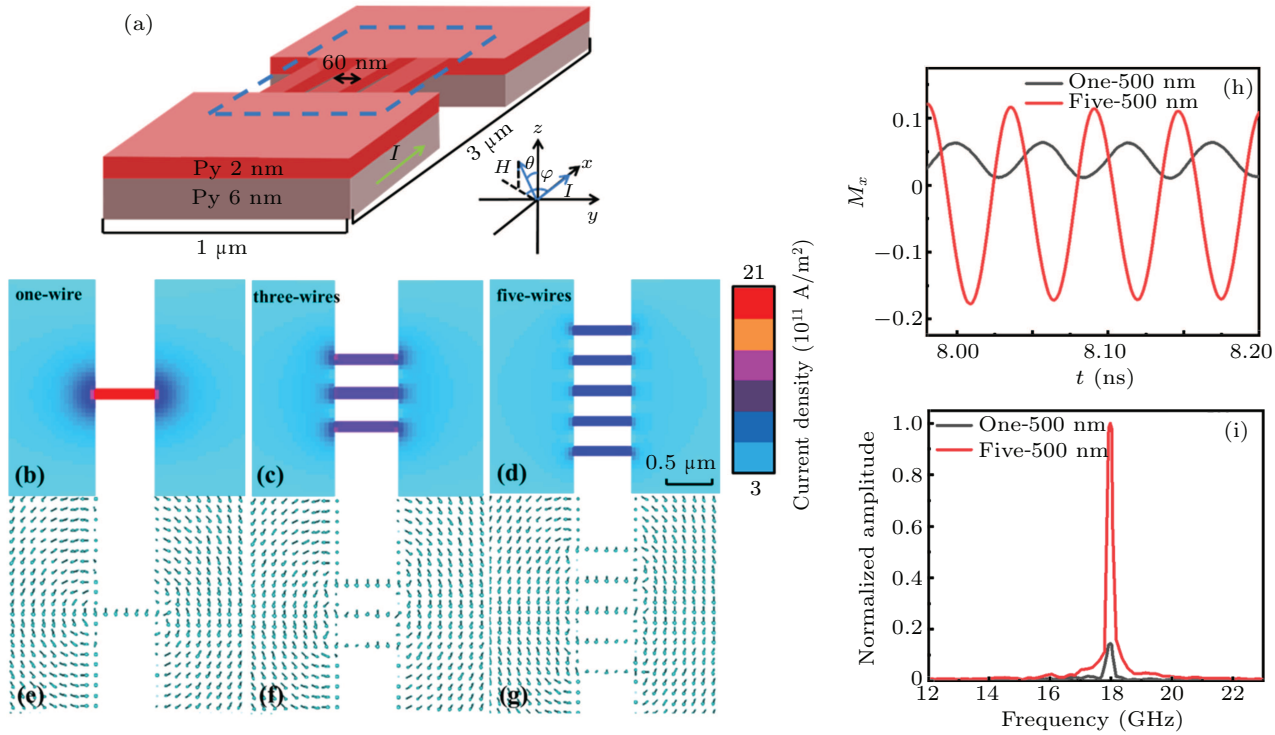


Fig. 1. (a) Schematic draw of the nanowire-based SHNO device; (b)–(g) The current density and Oersted field distribution of devices with nanowires number $N = 1, 3, 5$ under the same current intensity, respectively. (h) The temporal profiles of M_x in the blue dashed line area for devices with $N = 1$ and 5, respectively. (i) The frequency–domain spectra obtained from FFT analysis with data shown in Fig. 1(h).

Figures 1(b)–(d) show the current density distributions in the Pt layer of SHNOs in the region indicated by the dotted line in Fig. 1(a). Here the DC current is 1 mA for all devices. Obviously, that the current density in the nanowire dramatically decreases with increasing the number of nanowires. Figures 1(e)–1(g) show the distribution of the corresponding Oersted field. We can clearly see that the Oersted field appears a circular shape around the nanowires. Figures 1(h) and 1(i) show the magnetization precession in both times- and frequency-domains for SHNOs with one nanowire and five nanowires, respectively. Here, the currents are 0.8 mA and 4 mA for SHNOs with one nanowire and five nanowires, respectively. It is clear that the stable oscillation signal is generated in our structures, with frequencies close to 20 GHz. It is well known that the spin-wave of the nanowire spin oscillator will have two oscillation modes which is the bulk and edge modes, respectively.[32,39,40] The amplitude shown in Fig. 1(i) exhibits one peak, which is consistent with the previous study.[34] This result clearly indicated the edge mode closed to the bulk mode when the width of the nanowire decrese and then they can achieve synchronization with each other.[41,42] Moreover, the synchronization of them could be

further confirmed from the study of the influence of iDMI on this device in this paper. Furthermore, the linewidths of the oscillation signal Δf are about 280 MHz and 140 MHz for devices with one nanowire and five nanowires, respectively. We should mention several reasons responsible for the linewidth observed in Fig. 1(i). One reason might be the noise caused by the thermal fluctuation in our system.[22,35,43,44] Another reason might be the appearance of bulk and edge modes, further broadening the linewidth of the spectrum.[45,46] Also, the strong nonlinear frequency shift of the edge mode gives rise to nonlinear enhancement of the linewidth.[35] Moreover, for ferromagnetic/heavy metal (FM/HM) bilayer samples, the torque dissipation at the interface could be another source of the linewidth.[47] Therefore, to further decrease the linewidth for potential applications, we might focus on these issues. For example, we can fabricate high-quality samples with the interface sharper by epitaxial technique so the spin mixing conductance will be high. Subsequently, the spin current is more transparent at the interface. And then, the torque dissipation can be minimized, potentially resulting in the narrow linewidth. Moreover, the importance of the etching process is unquestionable. For nanowire-based devices, although the poor smoothness of the boundaries of the nanowire which is caused by the etching process will not lead to the appearance of new strong signals, it still brings about an increase in noise, a slight shift in frequency, and the increase in the linewidth.

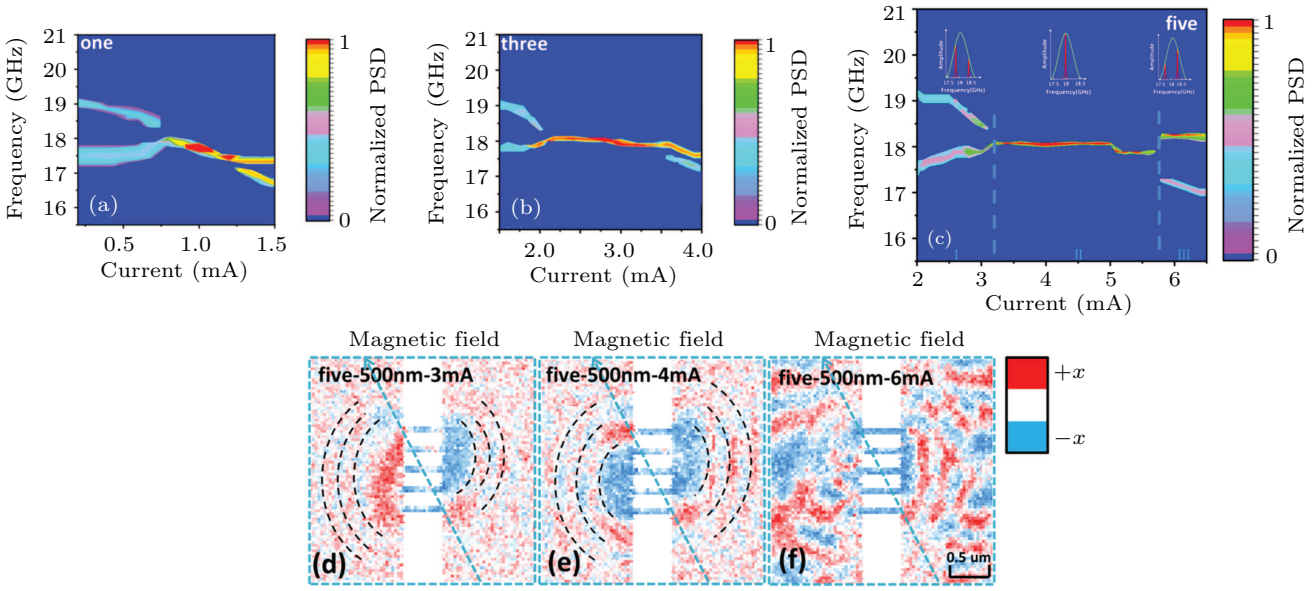


Fig. 2. (a)–(c) The spectra of frequency as a function of current for devices with one, three, five nanowires, respectively. I, II, and III show the schematic draws of spectra in the regions of detuning, synchronization, and disorder, respectively. (d)–(f) The spatial profiles of magnetization at different stages: (d) detuning, (e) synchronization, and (f) disorder. The black dashed lines represent the trajectories of the spin wave.

To further investigate the synchronization of nanowire-based devices driven by the current, we plot the frequency spectra as a function of current for different devices in Figs. 2(a)–2(c). It is clear that the spectra can be divided into three regions as the current increase. At the low current, the spectra clearly show two peaks. The one with decline tendency represents bulk mode, and the other with relatively flat represents edge mode. These separated two peaks indicate the detuning between bulk and edge modes. With the gradual increase of current, the spectra exhibit only one peak with very high intensity and narrow linewidth, indicating the device's synchronization. Further increasing the current intensity, the spectra exhibit two peaks again, indicating the disruption of synchronization. Here, we should point out that the spin-wave amplitude shown in Fig. 1(i) is greatly enhanced for the device with five nanowires. Therefore, we further focus on the SHNO with five nanowires to investigate the synchronization of the multiple devices in detail. Basically, as described above, we can divide the current range shown in Fig. 2(c) into three regions: (I) detuning region, (II) synchronization region, and (III) disorder region. Figures 2(d)–2(f) show the spatial profiles of magnetization with red and blue colors representing opposite directions of M_x, respectively. Here, we should mention that the self-oscillating bullet mode forms an ellipse shape due to the external magnetic field. In principle, we can treat it as a single device when the multiple devices are synchronized. In this case, the oscillation mode will exhibit an elliptical symmetry.[48] With the increase of the current, the multiple devices ignite the self-oscillation, but it is now in an asynchronous detuning state. The frequencies of bulk and edge modes have a great difference, as shown in the first inset in Fig. 2(c), and the phases of the magnetization precession in both sides of the dashed line shown in Fig. 2(d) are quite different and even opposite. When the current reaches about 3.2 mA, the frequency and phase of self-oscillation in multiple nanowires begin to lock-in, and the magnetization oscillation starts to synchronize. Eventually, the signal's amplitude significantly increases, and the linewidth greatly reduces (see the middle inset of Fig. 2(c)). In this case, the corresponding spatial profile of magnetization represents a symmetrical pattern

along the external field (dashed line), as shown in Fig. 2(e). However, when the current exceeds a certain critical value (5.8 mA in Fig. 2(c)), the spectra of frequency exhibit two peaks again, indicating the device in the stage of detuning (see the last inset of Fig. 2(c)). Meanwhile, the corresponding spatial profile of magnetization demonstrates a disordered behavior due to the large current (see Fig. 2(f)).

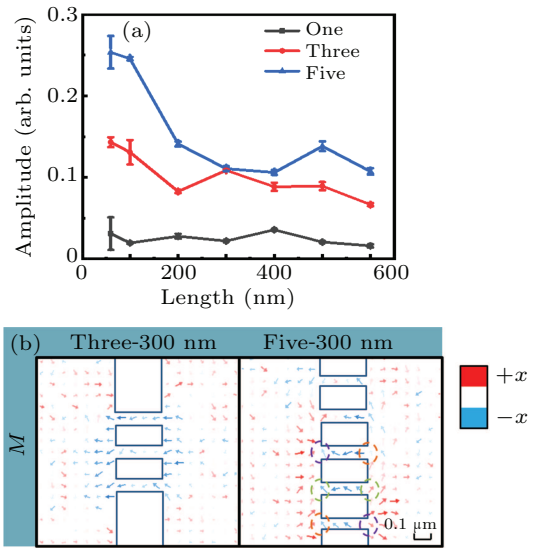


Fig. 3. (a) The FFT amplitude as a function of nanowires length for devices with nanowire number $N = 1$, 3, 5, respectively. (b) The spatial profiles of magnetization for devices with the length of nanowires being 300 nm. The dotted ovals indicate the regions of edge modes synchronized with each other in the devices with five nanowires.

In order to investigate the influence of the length of nanowires on synchronization, we further focus on the SHNO with the different numbers of nanowires $N = 1$, 3, and 5. As shown in Fig. 3(a), compared to the single nanowire, the amplitude of the spectra can be significantly improved for the synchronized multiple nanowires. With the increase of nanowires' length, the amplitude will decrease rapidly, indicating the weakening of synchronization due to the long distance of the oscillation cores of bulk and edge modes. This result agrees well with the previous study of nano-oscillators.[28] The ratio of amplitudes is 1:3.4:5.3 when the length of the nanowires is less than 100 nm, which is very close to the number of the nanowires (the power is proportional to the square value of the amplitude in our analysis system). The amplitude of the spectra will slightly fluctuate with the length of the nanowires. This is because the phase of spectra is dependent on the length of the nanowires, subsequently affecting the phase-locking of the observed spectra.[17] In particular, as shown in Fig. 3(a), when the length is 300 nm, the amplitudes of SHNO with three and five nanowires are almost identical. We further examine the spatial profiles of magnetization of these two samples. As illustrated in Fig. 3(b), the device with three nanowires can be completely synchronized and indicated by the arrow's color. However, only the three nanowires marked by the dotted ovals demonstrate synchronization for the device with five nanowires, while the other two are completely asynchronous. This behavior further demonstrates that the length of nanowires will be very critical during the synchronization of multiple devices.

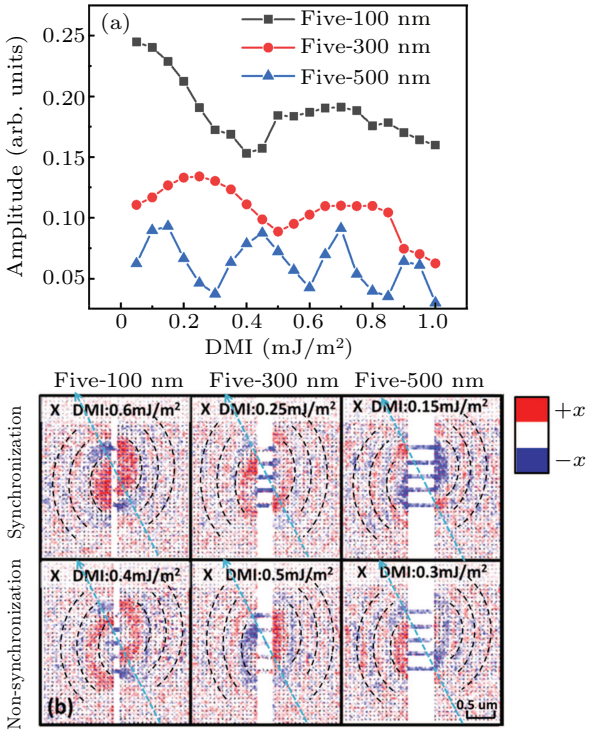


Fig. 4. (a) The FFT amplitude as a function of intensity of iDMI for five nanowire-based SHNO devices with different nanowires lengths. (b) The spatial profiles of magnetization in the stages of synchronization and non-synchronization. The blue dashed lines represent the projections of the external field in the film plane. The black dashed lines represent the trajectories of the spin wave.

It is well known that DMI can induce some special spin structures such as magnetic skyrmion lattices and spin spirals.[49–51] In particular, for FM/HM heterostructures with broken spatial inversion symmetry, the iDMI can be arisen due to the large spin-orbit coupling at the interface. Moreover, such an iDMI can be tuned with the electric field and further stabilize the magnetic skyrmion and domain walls in the Neel configuration with certain chirality.[52,53] In our structure of multiple devices, this iDMI will definitely exist due to the FM/HM interface. It might play an important role in the synchronization of multiple devices. We further investigate the influence of iDMI on the synchronization of nanowire-based SHNO devices. As shown in Fig. 4(a), it is clear that the amplitudes of spectra exhibit oscillations with the strength of DMI. This is because the iDMI affects the amplitude and the phase of the spin-wave, resulting in the modulation of spectra intensity during the synchronization. Another interesting point is that the period of oscillation of spectra intensity decreases with the increase of nanowires length, again indicating the length of nanowires plays an important role in the synchronization in multiple devices.[54] Moreover, the modulation ratio of the amplitude $\Delta A = A_{\max} - A_{\min}/A_{\max}$ can even reach about 100% in the device with a nanowires length of 500 nm. We further plot the magnetization spatial profiles of

synchronous and asynchronous states in Fig. 4(b). The synchronization in multiple devices can be modulated by introducing iDMI. This modulation result of IDMI also shows that the spin-waves come from the tuning of bulk and edge mode rather than the simple superposition of them. This result will definitely pave a new way to optimize SHNO devices for future application, for example, by funding iDMI with an electric field.[55,56]

3. Conclusions

In summary, we investigated the synchronization of SHNOs with the different numbers of nanowires devices. The synchronization can be obtained by tuning the frequency and phase of bulk and edge modes of spectra. For devices with multiple nanowires, we also need to tune the phase of spectra between these nanowires in order to synchronize the signals fully. The amplitude of synchronized spectra is remarkably enhanced with a very narrow linewidth for multiple devices. Moreover, the synchronization of multiple devices is strongly related to the length of nanowires, and the intensity of spectra almost exponentially delays with the length of the nanowires. Finally, we demonstrate that the iDMI can effectively modulate the synchronized spectra with a periodic oscillation. The modulation ratio can even reach about 100% by varying the strength of iDMI. This will be of great significance for developing spin logic devices.

Acknowledgements

Project supported by the National Basic Research Program of Natural Science Foundation of China (Grant Nos. 12074220, and 11627805) and the 111 Project (Grant No. B13029).

References

[1] Slonczewski J C 1996 *J. Magn. Magn. Mater.* **159** L1
[2] Berger L 1996 *Phys. Rev. B* **54** 9353
[3] Ralph D C and Stiles M D 2008 *J. Magn. Magn. Mater.* **320** 1190
[4] Kimura T, Sato T and Otani Y 2008 *Phys. Rev. Lett* **100** 066602
[5] Hamrle J, Kimura T, Otani Y, Tsukagoshi K and Aoyagi Y 2005 *Phys. Rev. B* **71**
[6] Fulara H, Zahedinejad M, Khymyn R, Awad A A, Muralidhar S, Dvornik M and Åkerman J 2019 *Sci. Adv.* **5** 8467
[7] Csaba G and Porod W 2013 *IEEE Trans. Magnet.* **49** 4447
[8] Yogendra K, Fan D, Jung B and Roy K 2016 *IEEE Trans. Electron Dev.* **63** 1674
[9] Demidov VE, Urazhdin S, Ulrichs H, Tiberkevich V, Slavin A, Baither D, Schmitz G, Demokritov SO 2012 *Nat. Mater.* **11** 1028
[10] Chen T, Dumas R K, Eklund A, Muduli P K and Åkerman J 2016 *IEEE* **104** 1919
[11] Cheng R, Xiao D and Brataas A 2016 *Phys. Rev. Lett* **116** 207603
[12] Demidov V E, Urazhdin S, Zholud A, Sadovnikov A V and Demokritov S O 2014 *Appl. Phys. Lett.* **105** 172410
[13] Giordano A, Carpentieri M, Laudani A, Gubbiotti G, Azzerboni B and Finocchio G 2014 *Appl. Phys. Lett.* **105** 042412
[14] Sharma A, Tulapurkar A A and Muralidharan B 2017 *Phys. Rev. Appl.* **8** 064014
[15] Li L Y, Chen L N, Liu R H and Du Y W 2020 *Chin. Phys. B* **29** 117102
[16] Chen L N, Urazhdin S, Du Y W and Liu R H 2019 *Phys. Rev. Appl.* **11** 064038
[17] Awad A A, Dürrenfeld P, Houshang A, Dvornik M, Iacocca E, Dumas R K and Åkerman J 2016 *Nat. Phys.* **13** 292
[18] Hache T, Li Y, Weinhold T, Scheumann B, Gonçalves F J T, Hellwig O, Fassbender J and Schultheiss H 2020 *Appl. Phys. Lett.* **116**
[19] Durrenfeld P, Awad A A, Houshang A, Dumas R K and Åkerman J 2017 *Nanoscale* **9** 1285
[20] Zahedinejad M, Mazraati H, Fulara H, Yue J, Jiang S, Awad A A and Åkerman J 2018 *Appl. Phys. Lett.* **112** 132404
[21] Sumito T, Tomohiro T, Romain L, Kay Y, Vincent C, Julie G, Akio F, Shinji Y and Hitoshi K 2018 *Sci. Rep.* **8** 13475
[22] Zahedinejad M, Awad A.A, Muralidhar S, Khymyn R, Fulara H, Mazraati H, Dvornik M and Åkerman J 2020 *Nat. Nanotechnol.* **15** 47
[23] Hamid M, Shreyas M, Seyyed R E, Mohammad Z, Seyed A B, Sunjae C, Ahmad A A, Mykola D and Johan Å 2018 arxiv: 1812.06350v1 [hep-ph]
[24] Mancoff F B, Rizzo N D, Engel B N and Tehrani S 2005 *Nature* **437** 393
[25] Kaka S, Pufall M R, Rippard W H, Silva T J, Russek S E and Katine J A 2005 *Nature* **437** 389
[26] Kenneth and Fink S 2000 *Phys. Rev. E* **61** 5080
[27] Elyasi M, Bhatia C S and Yang H 2015 *J. Appl. Phys.* **117**
[28] Kendziorczyk T and Kuhn T 2016 *Phys. Rev. B* **93**
[29] Li Q Y, Zhao D and Li Z D 2021 *Chin. Phys. B* **30** 017504
[30] Fu Q W, Li Y, Chen L N, Ma F S, Li H T, Xu Y B, Liu B, Liu R H and Du Y W 2020 *Chin. Phys. Lett.* **37** 087503
[31] Kang Y B, Lin F Y, Li K X, Tang J L, Hou X B, Wang D K, Fang X, Fang D, Wang X W and Wei Z P 2021 *Chin. Phys. B* **30** 078102
[32] Duan Z, Smith A, Yang L, Youngblood B, Lindner J, Demidov V E, Demokritov S O and Krivorotov I N 2014 *Nat. Commun.* **5** 5616
[33] Yang L, Verba R, Tiberkevich V, Schneider T, Smith A, Duan Z, Youngblood B, Lenz K, Lindner J, Slavin A N and Krivorotov I N 2015 *Sci. Rep.* **5** 16942
[34] Chen J R, Smith A, Montoya E A, Lu J G and Krivorotov I N 2020 *Commun. Phys.* **3**
[35] Slavin A and Tiberkevich V 2009 *IEEE Trans. Magn.* **45** 1875
[36] Slavin A and Tiberkevich V 2005 *Phys. Rev. Lett.* **95** 237201
[37] Consolo G, Lopez-Diaz L, Torres L and Azzerboni B 2007 *Phys. Rev. B* **75** 214428
[38] Arne V, Jonathan L, Mykola D, Mathias H, Felipe G S and Bartel V W 2014 *AIP Adv.* **4** 107133
[39] Bayer C, Jorzick J, Hillebrands B, Demokritov S O, Kouba R, Bozinoski R, Slavin A N, Guslienko K Y, Berkov D V, Gorn N L and Kostylev M P 2005 *Phys. Rev. B* **72**
[40] Park J P, Eames P, Engebretson D M, Berezovsky J and Crowell P A 2002 *Phys. Rev. Lett.* **89** 277201
[41] Awad A A, Houshang A, Zahedinejad M, Khymyn R and Kerman J 2020 *Appl. Phys. Lett.* **116** 232401
[42] Duan Z, Krivorotov I N, Arias R E, Reckers N, Stienen S and Lindner Jürgen 2015 *Phys. Rev. B* **92** 104424
[43] Sankey J C, Krivorotov I N, Kiselev S I, Braganca P M, Emley N C, Buhrman R A and Ralph D C 2005 *Phys. Rev. B* **72** 224427
[44] Boone C, Katine J A, Childress J R, Zhu J, Cheng X and Krivorotov I N 2009 *Phys. Rev. B* **79** 140404
[45] Krivorotov I N, Emley N C, Buhrman R A and Ralph D C 2008 *Phys. Rev. B* **77** 054440
[46] Iacocca E, Heinonen O, Muduli P K and Åkerman J 2014 *Phys. Rev. B* **89** 054402
[47] Šimánek E and Heinrich B 2003 *Phys. Rev. B* **67**
[48] Kendziorczyk T and Kuhn T 2016 *Phys. Rev. B* **93** 134413
[49] Rohart S and Thiaville A 2013 *Phys. Rev. B* **88** 184422
[50] Gayles J, Freimuth F, Schena T, Lani G, Mavropoulos P, Duine R A, Blügel S and Sinova J Y 2015 *Phys. Rev. Lett.* **115** 036602
[51] Yang J, Li J, Lin L Z and Zhu J J 2020 *Chin. Phys. Lett.* **37** 087501
[52] Frank F, Robert B, Yuriy M and Achim R 2013 *Phys. Rev. B* **88** 214409
[53] Yang H X, Olivier B, Vincent C, Albert F and Mairbek C 2018 *Sci. Rep.* **8** 12356
[54] Yang L, Philipp D, Ruan X Z, Liu W Q, He L, Xu Y B and Zhou Y 2017 *IEEE Magn. Lett.* **8** 1
[55] Zhang W J, Zhong H R. Zang R X, Zhang Y, Yu S S, Han G B, Liu G L, Yan S S, Kang S S and Li M 2018 *Appl. Phys. Lett.* **113** 122406
[56] Suwardy J, Nawaoka K, Cho, J, Goto M, Suzuki Y and Miwa S 2018 *Phys. Rev. B* **98** 144432